SITE-BASED STOCHASTIC GROUND MOTION SIMULATION BASED ON WHITE NOISE MODIFICATION

SAYED M. S. HUSSAINI
PhD student
University of Minho

SHAGHAYEGH KARIMZADEH
Researcher
University of Minho

PAULO B. LOURENÇO
Full Professor
University of Minho

ABSTRACT
This paper presents an innovative approach to site-based stochastic ground motion simulation, aiming to capture essential characteristics of real accelerograms through the modification of a white noise process. Traditional site-based simulation methods often fall short in replicating the intricacies of seismic events, or they are too complex to be used in general engineering practice. To address this, we introduce a multi-step process that enhances the fidelity of synthetic ground motions. Our approach includes frequency-dependent filtering, amplitude modulation, temporal variation modeling, and station-specific adaptation, resulting in synthetic motions that closely resemble real seismic events. Comparative analysis with actual accelerograms demonstrates the effectiveness of our method in replicating crucial ground motion features. This novel approach offers a practical and user-friendly tool for incorporating stochastic simulations into seismic hazard assessment and structural design, making a valuable contribution to the field of earthquake engineering.

SUMÁRIO
Este artigo apresenta uma abordagem inovadora para a simulação estocástica do movimento do solo com base no local, com o objetivo de capturar características essenciais de acelerogramas reais através da modificação de um processo de ruído branco. Métodos tradicionais de simulação baseados no local frequentemente falham em replicar as complexidades de eventos sísmicos, ou são muito complexos para serem utilizados na prática geral de engenharia. Para lidar com isso, introduzimos um processo de vários passos que aprimora a fidelidade dos movimentos sísmicos sintéticos. Nossa abordagem inclui filtragem dependente da frequência, modulação de amplitude, modelagem de variação temporal e adaptação específica da estação, resultando em movimentos sintéticos que se assemelham de perto a eventos sísmicos reais. A análise comparativa com acelerogramas reais demonstra a eficácia de nosso método em replicar características cruciais do movimento do solo. Esta abordagem inovadora oferece uma ferramenta prática e de fácil utilização para incorporar simulações estocásticas na avaliação de risco sísmico e no projeto estrutural, fazendo uma contribuição valiosa para o campo da engenharia sísmica.

Keywords: Earthquake ground motion, Site-based stochastic approach, White noise modification, Seismic hazard assessment, Synthetic ground motion.

1. INTRODUCTION

Recent seismic occurrences, as exemplified by the significant 2023 earthquakes in Turkey, highlight the profound havoc that earthquakes can inflict, leading to the loss of life and extensive structural damage. This recognition has heightened the significance of evaluating structural vulnerability, and in response, computational techniques have emerged as pivotal instruments that present both new possibilities and challenges.

The nonlinear behavior of structures, a critical aspect in earthquake engineering, is now more effectively explored through advanced numerical methodologies, notably the finite element method (FEM) [1–3]. However, the efficacy of such analyses hinges on the availability of comprehensive time-series data for ground motions. This prerequisite becomes particularly vital in regions lacking seismic stations or limited historical data on large- and moderate-magnitude earthquakes capable of causing substantial damage.

While the global proliferation of strong-motion networks has expanded, seismic gaps persist in various regions, limiting the pool of available recorded strong ground motions. This scarcity poses challenges in characterizing specific analysis conditions or envisioning potential design scenarios. Engineers often address this limitation by selecting recorded motions with seismological characteristics divergent from the site of interest, subsequently adjusting them through scaling or spectrum matching [4,5]. However, such controversial approaches introduce complexities and may compromise the correlation between recorded ground motion characteristics and their original physical conditions, potentially resulting in the generation of motions with unrealistic features [6,7].

A more reliable alternative involves the performance of ground motion simulations that faithfully incorporate key features of real earthquakes and align with the specific physical conditions of interest. This approach is crucial for achieving a realistic estimation of seismic demand, especially when sophisticated nonlinear structural models are considered. The robustness and validity of these simulation methodologies have been globally acknowledged, finding extensive utilization and validation in seismology and various engineering disciplines [8–11].

Categorically, ground motion simulation techniques can be classified into three main groups [12]. The initial category employs a physical approach characterized by modeling fault rupture and transmitting the resultant waves to the target site. This specific category is commonly known as physics-based or deterministic source-based methods [13]. These sophisticated methods are not widely adopted in engineering practice due to their substantial demands for high computational resources and a comprehensive understanding of the ground media. Achieving such proficiency necessitates thorough engagement in seismological studies.

The second category encompasses stochastic methods, which are either empirically calibrated or fitted to recorded ground motions [14–16]. As for the third class, hybrid methods combine the features of the first two to produce comprehensive synthetic ground motions [17]. Stochastic methods can incorporate the physical attributes of the earthquake source, along with path and site effects, implicitly through their formulations, parameters, and empirical calibration. These methods can be broadly classified into two approaches: source-based and site-based [13,14]. In the source-based stochastic approach, the earthquake source's theoretical spectrum is shaped and scaled, incorporating the influences of path and site described in terms of seismological parameters [15,16,18]. However, these region-specific parameters can vary significantly between regions, constraining their application in engineering practice [19]. In contrast, site-based stochastic approaches directly simulate a recorded ground motion at a specific site by modifying a stochastic process that captures crucial features of the observed motions. Typically, these approaches require fewer parameters and are less computationally expensive compared to source-based or hybrid simulations. These

attributes, combined with their simplicity, render site-based models more attractive for engineering applications.
Following [13], site-based stochastic models in literature can be categorized into five classes; 1) Filtered white-noise processes [14,20–23], 2) Filtered Poisson pulse train [24], 3) Auto-regressive moving average processes [25], 4) Spectral representations using short-time Fourier or wavelet transforms [26–29], 5) Machine learning non-parametric processes such as Gaussian process regression [30,31].

The main issue in site-based stochastic models is that their parameters are mathematical and lack physical considerations. Most of these methods underperform in low-frequency ranges. To improve their low-frequency performance, an additional forward directivity velocity pulse model can be combined [21,23]. However, it comes at the cost of increased complexity and number of parameters, which is not attractive to engineering practice.

This paper is built upon a fully non-stationary site-based stochastic method based on white-noise modification. Efforts are made to keep the stochastic model as simple as possible and attractive to engineering practice. The proposed stochastic model is capable of simulating far-field and near-fault pulse-like ground motions without the need for supplementary models. The paper starts with a summary of a fully non-stationary stochastic model and a modification of the model formulation. A new filter function is developed to improve capturing the frequency content of recorded ground motions, particularly near-fault pulse-like motions. To assess the model performance, distinct recorded ground motions with various scenarios are selected and simulated. The assessment of simulations is conducted in terms of ground motion time-series and spectral acceleration at five percent damping.

2. IMPROVING A FULLY NON-STATIONARY STOCHASTIC MODEL

2.1. Improved Model Formulation

This study improves a fully non-stationary stochastic model proposed by [14]. This model accounts for the temporal and spectral non-stationarities separately. This is a key benefit in parameter calibration and interpretation. The model formulation is expressed as:

$$x(t) = q(t, \alpha)\left\{\frac{1}{\sigma_h(t)}\int_{-\infty}^{t} h\big(t-\tau, \lambda(\tau)\big)w(\tau)d\tau\right\} \quad 1$$

where $q(t, \alpha)$ with shape parameters α, is a modulating function to account for temporal non-stationarity, $w(\tau)$ is a white-noise process, $h\big(t-\tau, \lambda(\tau)\big)$ is the shifted filter with parameters $\lambda(\tau)$, and $\sigma_h^2(t) = \int_{-\infty}^{t} h^2\big(t-\tau, \lambda(\tau)\big)d\tau$ is the variance of the integral process. Normalization by $\sigma_h(t)$ leads to a unit variance process denoted by the term inside the curved brackets. This term is a filtered white noise process that accounts for spectral non-stationarity. The described stochastic model first filters a white noise process to capture the frequency content observed in a ground motion. Then, the model modulates the process to account for the distribution of energy over time. As pointed out by [32], this order of modulating after filtering affects the low-frequency components as measured by the Fourier amplitude spectrum. Since the modulating function is typically a smooth function of time, its Fourier amplitude spectrum exhibits peaks at very low-frequency components. Therefore, modulating after filtering often distorts the low-frequency components. In other words, the stochastic model always requires additional high-pass filtering to remove the unwanted low-frequency components. This is necessary to remove the velocity and displacement residuals and correct the long-period spectral acceleration. The study by [14] employed a critically damped second-order oscillator for high-pass filtering.

To address the above issue, we modify the model formulation while preserving the advantage of the model. The proposed modified model is expressed as:

$$x(t) = \int_{-\infty}^{t} q(\tau, \alpha) w(\tau) \frac{\delta(t-\tau) * h\big(t, \lambda(\tau)\big)}{\sigma_h(t)} d\tau \qquad 2$$

where $x(t)$ is the final acceleration process, $q(t, \alpha)$ is a deterministic modulating function, $w(t)$ is a zero mean unit variance Gaussian white noise process, $h(t, \lambda(\tau))$ is a band-pass filter, and $\sigma_h^2(t) = \int_{-\infty}^{t} h^2\big(t-\tau, \lambda(\tau)\big) dt$ is a term that normalizes the filter function. This normalization ensures that the temporal non-stationarity is affected solely by the modulating function. On the other hand, the normalized filter function controls the spectral non-stationarity of the process. Note that the normalization terms in Equations 1 and 2 are integrated with respect to $d\tau$ and dt, respectively.

2.2. Proposed Filter Function

A widely used filter function in the site-based stochastic model in Equation 1, is the pseudo-acceleration response of an underdamped single degree of freedom (SDOF) linear system [14]. This filter is expressed as:

$$h\big(t-\tau, \lambda(\tau)\big) = \frac{\omega(\tau)}{\sqrt{1-\zeta^2(\tau)}} e^{-\zeta(\tau)\omega(\tau)(t-\tau)} \sin\Big(\omega(\tau)\sqrt{1-\zeta^2(\tau)}(t-\tau)\Big) \qquad 3$$

where $\lambda(\tau) = (\zeta(\tau), \omega(\tau))$ denotes damping ratio and frequency as the filter parameters, respectively. The frequency parameter of this filter accounts for the evolutionary predominant frequency of ground motions, and the damping ratio accounts for the frequency bandwidth. The Fourier amplitude spectrum (FAS) of this filter, as shown in Fig. 1 for a value of $\zeta(\tau)$ and $\omega(\tau)$, indicates clearly that the zero-frequency amplitude in FAS that is equal to the mean level of the process is not zero. Therefore, the final acceleration is not zero-mean, and the velocity and displacement time-series have residuals. Therefore, high pass filtering is still required to address this issue. However, high-pass filtering removes the low-frequency components and their associated energy from the process. This means the final process underestimates the total energy. This restricts the stochastic model in Equation 1 to only far-field ground motions where low-frequency contents are not significant in terms of energy. A new filter function is proposed to avoid this average bias in the total energy of the final process and improve the capability of the model. This new filter attempts to remove the zero-frequency amplitude and the mean level from the process. Therefore, high pass filtering is not required anymore.

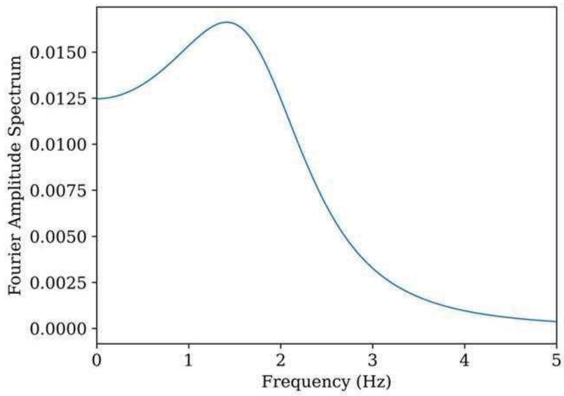

Fig. 1 Fourier Amplitude spectrum of the filter function for $\zeta = 0.5$ and $\omega = 2\ Hz$.

The new filter function is based on sequential filtering of the Pseudo acceleration and acceleration response of an SDOF system. The proposed filter function is expressed as:

$$h(t, \lambda(\tau)) = h_l(t, \lambda_l(\tau)) * h_u(t, \lambda_u(\tau)) \quad 4$$

$$h_l(t, \lambda_l(\tau)) = \frac{1}{\omega_l(\tau)^2} \frac{d^2}{dt^2} \left[h_u(t, \lambda_l(\tau)) \right] \quad 5$$

where $h_u(t, \lambda(\tau))$ is the filter function in Equation 3. Fig. 2 illustrates the FAS of the proposed filter function where a frequency bandwidth is delimited by the upper and lower corner frequencies. Moreover, the zero-frequency amplitude is zero, indicating a mean-free process in which it does not require high-pass filtering. It is important to note that the proposed filter function can mitigate the surplus of low frequencies in the model in Equation 1. However, to address the drawbacks, the proposed filter should be employed within the improved model in Equation 2.

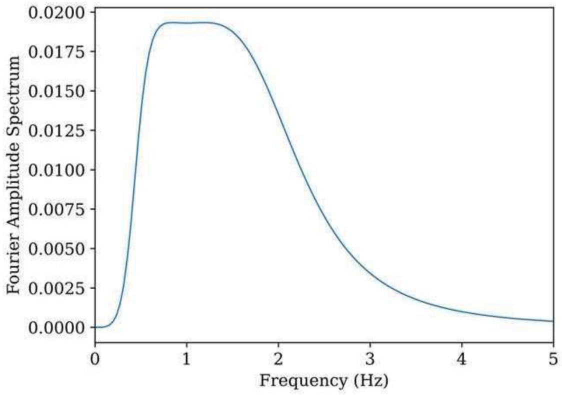

Fig. 2 Fourier Amplitude spectrum of the proposed filter function for $\zeta = 0.5$ and $\omega_l = 0.5\ Hz$ and $\omega_u = 2\ Hz$.

3. IDENTIFICATION OF MODEL PARAMETERS

3.1. Parameter identification procedure

Following [14], we adopt a Gamma modulating function initially proposed by [33] to account for temporal non-stationarity. The Gamma function is expressed as:

$$q(t, \alpha) = a_0 t^{a_1} e^{-\alpha_2 t} \quad 6$$

where a_0, a_1 and a_2 are the shape parameters. To obtain the parameters of the modulating function, the cumulative energy of the model is fitted to the same of a target accelerogram according to [14].

For the filter parameters, we employ a linear functional form for simplicity as below:

$$\omega_l(\tau) = \omega_{l_0} - \frac{\omega_{l_0} - \omega_{l_n}}{t_n} \tau \quad 7$$

$$\omega_u(\tau) = \omega_{u_0} - \frac{\omega_{u_0} - \omega_{u_n}}{t_n} \tau \quad 8$$

$$\zeta(\tau) = \zeta_0 - \frac{\zeta_0 - \zeta_n}{t_n} \tau \quad 9$$

The filter parameters (ω_{l_0}, ω_{l_n}, ω_{u_0}, ω_{u_n}, ζ_0, ζ_n) are identified by fitting the cumulative counts of zero-level up-crossing of the acceleration and its corresponding displacement as well as the cumulative counts of positive minima and negative maxima of the acceleration process to the same measurements of a target accelerogram as described in [14].

3.2. Model parameters for selected target accelerograms

Using the procedure in the previous section, we identify model parameters for two selected accelerograms. As shown in Table 1, selected accelerograms encompass component 90 of the Northridge-01 1994 earthquake recorded at the 116th Street School station (NGA RSN 984), the pulse-like component 0 of the Imperial Valley-06 1979 earthquake recorded at El Centro-Meloland Geotechnical Array station (NGA RSN 171). Repi, Rjb, and Rrup are epicentral, Joyner-Boore, and rupture distance metrics and Vs30 is the average shear wave velocity at the top 30m depth of soil.

Table 1 Seismological characteristics of the target accelerograms

NGA RSN	Magnitude	Mechanism	Repi (km)	Rjb (km)	Rrup (km)	Vs30 (m/sec)
984	6.69	Reverse	41	36.39	41.17	301
171	6.53	Strike-slip	19.44	0.07	0.07	264

Fig. *3* illustrates the cumulative energy of the model when fitting to the target accelerograms. It is clear that the Gamma function can easily account for the temporal distribution of energy where the energy arrives in a single strong motion phase. The identified parameters of the modulating function are shown in Table 2.

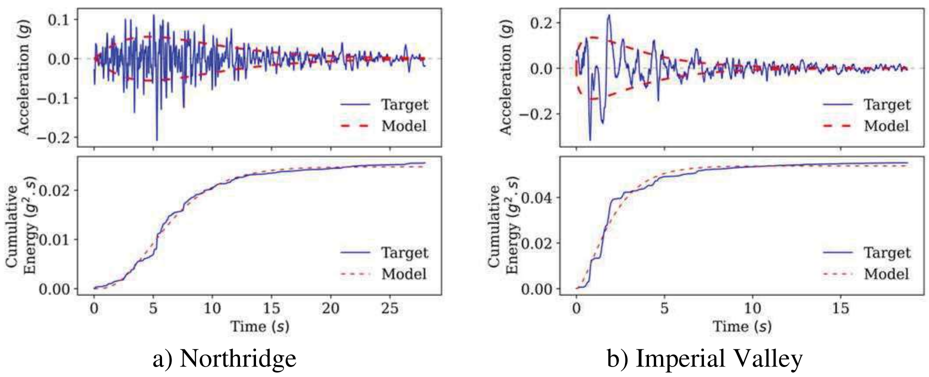

Fig. 3 Cumulative energy of the target accelerograms and the fitted models.

Table 2 Parameters of the modulating function fitted to target accelerograms.

NGA RSN	Modulating function parameters		
	a_0	a_1	a_2
984	0.03	1.17	0.25
171	0.2	0.37	0.41

Fig. 4 illustrates the cumulative counts of zero-level up-crossing of acceleration and its corresponding displacement time-series and the same of the target accelerograms. Similarly, Fig. 5 shows the cumulative count of positive minima and negative maxima (local extrema) of the acceleration process and the target accelerograms. It is evident the linear functional form of filter parameters can effectively capture the time variation of these metrics. In Imperial Valley ground motion, the rate of zero crossing, which is the slope of the curve in Fig. 4, is initially low and then increases over time in contrast to the Northridge. The filter parameters are shown in Table 3.

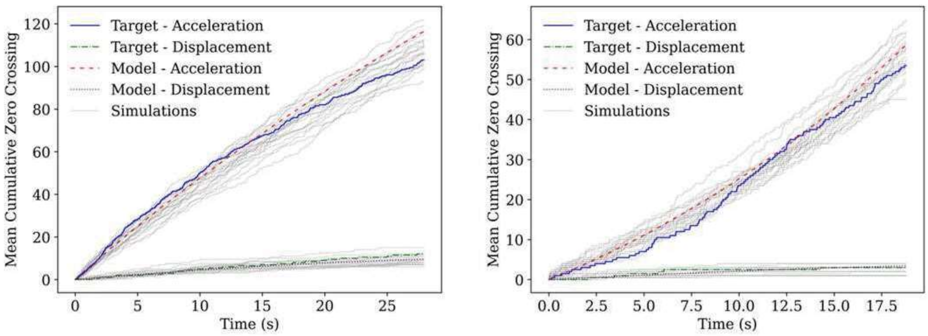

a) Northridge b) Imperial Valley

Fig. 4 Cumulative number of zero-level up-crossings of the target accelerograms and the fitted models.

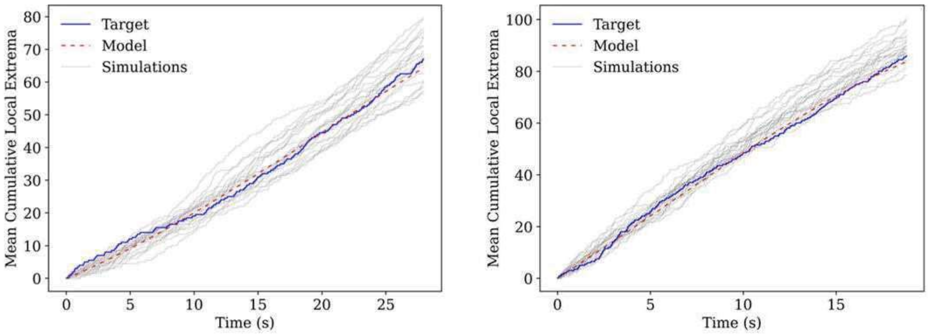

a) Northridge b) Imperial Valley

Fig. 5 Cumulative number of positive minima and negative maxima (local extrema) of the target accelerograms and the fitted models.

Table 3 Parameters of the filter function fitted to target accelerograms.

NGA RSN	Frequency parameters (Hz)				Damping ratio parameters	
	ω_{h_0}	ω_{h_n}	ω_{l_0}	ω_{l_n}	ζ_0	ζ_n
984	5.7	1.5	0.48	0.38	0.44	2.18
171	1.4	4.6	0.27	0.1	1.2	0.25

4. VALIDATION AND SIMULATION ASSESSMENT

Before applying simulations in engineering applications, it is imperative to verify the stochastic ground motion model. This validation is essential to confirm that the model effectively captures the essential features of recorded ground motions, thereby ensuring the credibility of synthetic motions for engineering purposes. This paper, in accordance with the literature [34–37], compares the ground motion time-series, the elastic response spectra, and the Fourier amplitude spectrum of the target accelerograms with those of the fitted stochastic model to verify the improved model.

Given the identified model parameters, the acceleration time-series can be obtained directly without any post-processing. Fig. 6 to Fig. 8 illustrate the acceleration, velocity, and displacement time-series of the target motions and two corresponding alternative simulations. It is evident that the improved model simulates motions that resemble the recorded time-series in terms of the overall waveform, intensity level, duration, frequency content, pulse timing, and pulse intensity without considering additional explicit constraints on these near-fault features.

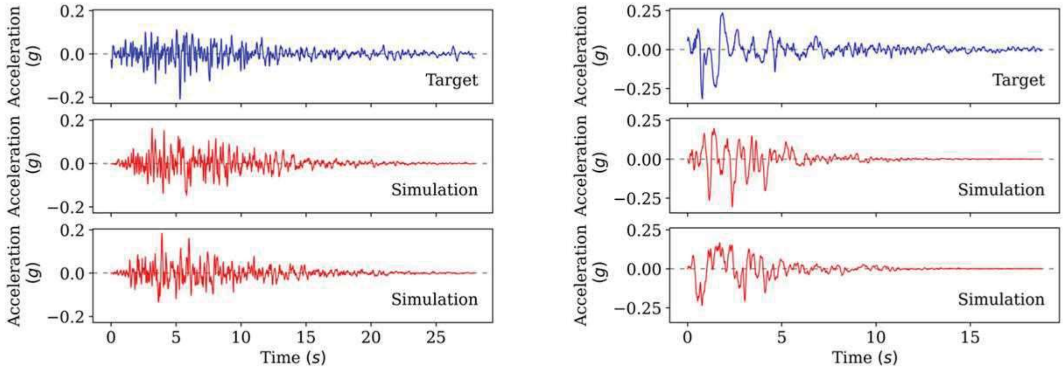

a) Northridge b) Imperial Valley

Fig. 6 Target accelerograms and two alternative simulations using the fitted model.

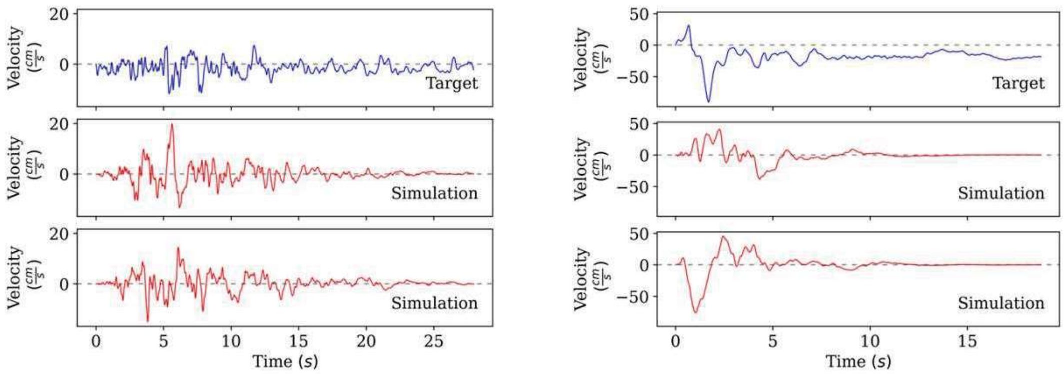

a) Northridge b) Imperial Valley

Fig. 7 Target Velocity time-series and two alternative simulations using the fitted model.

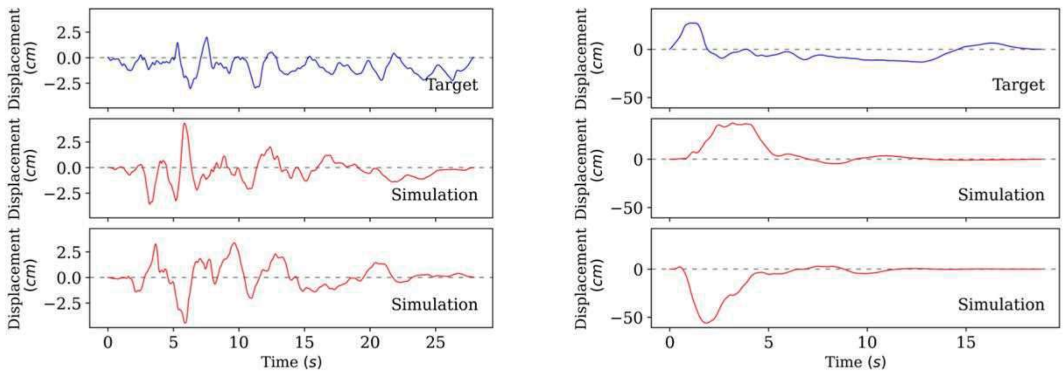

a) Northridge b) Imperial Valley

Fig. 8 Target displacement time-series and two alternative simulations using the fitted model.

As mentioned before, the proposed improved model avoids the average bias in the total energy of the target motions. Fig. 9 shows the cumulative energy of target motions and 20 alternative simulations. As can be seen, the average of the simulation matches the target motion, and there is no average bias in the energy build-up.

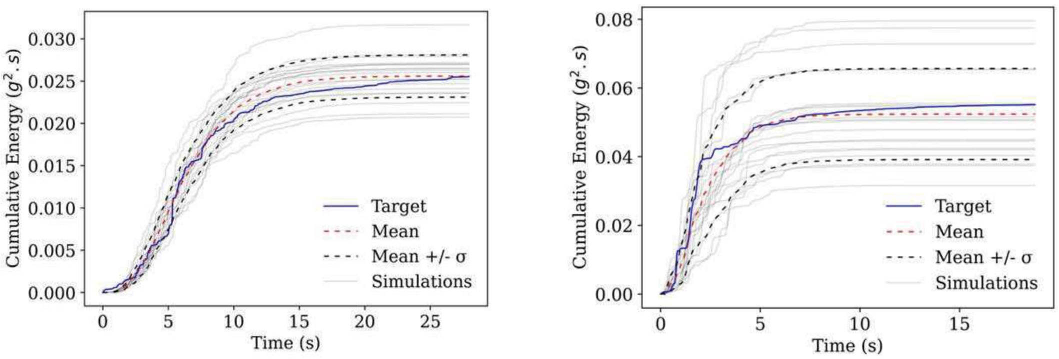

a) Northridge b) Imperial Valley

Fig. 9 Cumulative energy of target accelerograms and 20 alternative simulations using the fitted model.

To facilitate additional comparison, Fig. 10 depicts the spectral acceleration (SA) at 5% damping for both the target accelerograms and 20 corresponding alternative simulations. Notably, the SA of the target motions consistently falls within the ranges covered by those of the simulated motions across various period ranges. Hence, it is reasonable to regard the target motions as a single alternative realization of the stochastic model under the specified parameters.

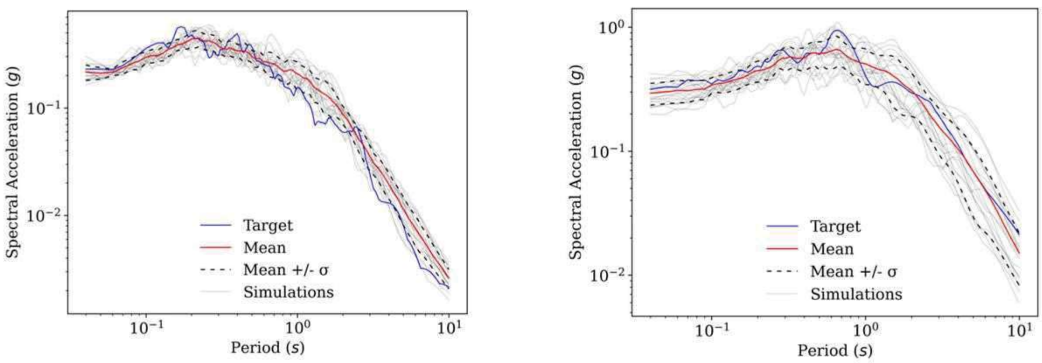

a) Northridge b) Imperial Valley

Fig. 10 Spectral acceleration of target accelerograms and 20 alternative simulations using the fitted model.

5. CONCLUSION

This paper improves the frequency content of a fully non-stationary stochastic site-based model. The proposed improvements include modification of the model formulation and introducing a new filter function. These improvements enable the simulation of near-fault pulse-like ground motion in addition to the far-field motions. Moreover, the additional post-processing step required in previous stochastic site-based models in the literature is omitted, leading to energy bias-free synthetic ground motions.

An in-depth description of the model application is presented, employing two specific target accelerograms with far-field and near-fault earthquake and site characteristics, including Northridge 1994 and Imperial Valley 1979 earthquakes. The stochastic model's validation involves visually comparing time-series data for acceleration, velocity, and displacement, along with examining elastic spectral acceleration. The analysis demonstrates that given identified parameters, the recorded motion can be regarded as a single realization of the stochastic model for that specific earthquake scenario which can be used in conjunction or in lieu of real recorded ground motions.

6. ACKNOWLEDGMENTS

The authors extend their appreciation to Dr. Sanaz Rezaeian for her invaluable insights and guidance throughout the development of this research.

7. FUNDING

This work was partly financed by FCT/MCTES through national funds (PIDDAC) under the R&D Unit ISISE under reference UIDB/04029/2020, and under the Associate Laboratory Advanced Production and Intelligent Systems ARISE under reference LA/P/0112/2020. This study has been partly funded by the STAND4HERITAGE project that has received funding from the European Research Council (ERC) under the European Union's Horizon 2020 research and innovation program (Grant agreement No. 833123), as an Advanced Grant. This work is partly financed by national funds through FCT - Foundation for Science and Technology, under grant agreement UI/BD/153379/2022 attributed to the first author.

8. REFERENCES

[1] Funari MF, Silva LC, Savalle N, Lourenço PB. A CONCURRENT MICRO/MACRO FE-MODEL OPTIMIZED WITH A LIMIT ANALYSIS TOOL FOR THE ASSESSMENT OF DRY-JOINT MASONRY STRUCTURES. Int J Multiscale Comput Eng 2022;20:65–85. https://doi.org/10.1615/INTJMULTCOMPENG.2021040212.

[2] Valente M, Milani G. Non-linear dynamic and static analyses on eight historical masonry towers in the North-East of Italy. Eng Struct 2016;114:241–70. https://doi.org/10.1016/J.ENGSTRUCT.2016.02.004.

[3] Karimzadeh S, Funari MF, Szabó S, Hussaini SMS, Rezaeian S, Lourenço PB. Stochastic simulation of earthquake ground motions for the seismic assessment of monumental masonry structures: Source-based vs site-based approaches. Earthq Eng Struct Dyn 2024;53:303–30. https://doi.org/10.1002/eqe.4012.

[4] Watson-Lamprey J, Abrahamson N. Selection of ground motion time series and limits on scaling. Soil Dynamics and Earthquake Engineering 2006;26:477–82. https://doi.org/10.1016/j.soildyn.2005.07.001.

[5] Hancock J, Watson-Lamprey J, Abrahamson NA, Bommer JJ, Markatis A, McCoyh E, et al. An improved method of matching response spectra of recorded earthquake ground motion using wavelets. Journal of Earthquake Engineering 2006;10:67–89. https://doi.org/10.1080/13632460609350629.

[6] Naeim F, Lew M. On the use of design spectrum compatible time histories. Earthquake Spectra 1995;11:111–27. https://doi.org/10.1193/1.1585805.

[7] Luco N, Bazzurro P. Does amplitude scaling of ground motion records result in biased nonlinear structural drift responses? Earthq Eng Struct Dyn 2007;36:1813–35. https://doi.org/10.1002/eqe.695.

[8] Rezaeian S, Hartzell S, Sun X, Mendoza C. Simulation of earthquake ground motions in the eastern United States using deterministic physics-based and site-based stochastic approaches. Bulletin of the Seismological Society of America 2017;107:149–68. https://doi.org/10.1785/0120160031.

[9] Fayaz J, Rezaeian S, Zareian F. Evaluation of simulated ground motions using probabilistic seismic demand analysis: CyberShake (ver. 15.12) simulations for Ordinary Standard Bridges. Soil Dynamics and Earthquake Engineering 2021;141:106533. https://doi.org/10.1016/j.soildyn.2020.106533.

[10] Rezaeian S, Der Kiureghian A. Simulation of orthogonal horizontal ground motion components for specified earthquake and site characteristics. Earthq Eng Struct Dyn 2012;41:335–53. https://doi.org/10.1002/eqe.1132.

[11] Arslan Kelam A, Karimzadeh S, Yousefibavil K, Akgün H, Askan A, Erberik MA, et al. An evaluation of seismic hazard and potential damage in Gaziantep, Turkey using site specific models for sources, velocity structure and building stock. Soil Dynamics and Earthquake Engineering 2022;154:107129. https://doi.org/10.1016/j.soildyn.2021.107129.
[12] Douglas J, Aochi H. A survey of techniques for predicting earthquake ground motions for engineering purposes. Surv Geophys 2008;29:187–220. https://doi.org/10.1007/s10712-008-9046-y.
[13] Rezaeian S, Sun X. Stochastic ground motion simulation. Encyclopedia of Earthquake Engineering, Berlin, Heidelberg: Springer Berlin Heidelberg; 2014, p. 1–15. https://doi.org/10.1007/978-3-642-36197-5_239-1.
[14] Rezaeian S, Der Kiureghian A. A stochastic ground motion model with separable temporal and spectral nonstationarities. Earthq Eng Struct Dyn 2008;37:1565–84. https://doi.org/10.1002/eqe.831.
[15] Boore DM. Simulation of ground motion using the stochastic method. Pure Appl Geophys 2003;160:635–76. https://doi.org/10.1007/PL00012553.
[16] Boore DM. Comparing stochastic point-source and finite-source ground-motion simulations: SMSIM and EXSIM. Bulletin of the Seismological Society of America 2009;99:3202–16. https://doi.org/10.1785/0120090056.
[17] Graves RW, Pitarka A. Broadband ground-motion simulation using a hybrid approach. Bulletin of the Seismological Society of America 2010;100:2095–123. https://doi.org/10.1785/0120100057.
[18] Motazedian D. Stochastic finite-fault modeling based on a dynamic corner frequency. Bulletin of the Seismological Society of America 2005;95:995–1010. https://doi.org/10.1785/0120030207.
[19] Stafford PJ, Sgobba S, Marano GC. An energy-based envelope function for the stochastic simulation of earthquake accelerograms. Soil Dynamics and Earthquake Engineering 2009;29:1123–33. https://doi.org/10.1016/j.soildyn.2009.01.003.
[20] Alamilla J, Esteva L, García-Pérez J, Díaz-López O. Evolutionary properties of stochastic models of earthquake accelerograms: Their dependence on magnitude and distance. Journal of Seismology 2001 5:1 2001;5:1–21. https://doi.org/10.1023/A:1009892002555.
[21] Waezi Z, Balzadeh S. Simulation of near-field pulse-like ground motions using a correlated bimodal fractional stochastic model. Soil Dynamics and Earthquake Engineering 2022;161:107434. https://doi.org/10.1016/j.soildyn.2022.107434.
[22] Waezi Z, Rofooei FR, Hashemi MJ. A multi-peak evolutionary model for stochastic simulation of ground motions based on time-domain features. Journal of Earthquake Engineering 2021;25:343–79. https://doi.org/10.1080/13632469.2018.1518279.
[23] Dabaghi M, Der Kiureghian A. Stochastic model for simulation of near-fault ground motions. Earthq Eng Struct Dyn 2017;46:963–84. https://doi.org/10.1002/eqe.2839.
[24] Lin YK. On random pulse train and its evolutionary spectral representation. Probabilistic Engineering Mechanics 1986;1:219–23. https://doi.org/10.1016/0266-8920(86)90015-9.
[25] Sgobba S, Stafford PJ, Marano GC, Guaragnella C. An evolutionary stochastic ground-motion model defined by a seismological scenario and local site conditions. Soil Dynamics and Earthquake Engineering 2011;31:1465–79. https://doi.org/10.1016/j.soildyn.2011.05.014.
[26] Yamamoto Y, Baker JW. Stochastic model for earthquake ground motion using wavelet packets. Bulletin of the Seismological Society of America 2013;103:3044–56. https://doi.org/10.1785/0120120312.
[27] Pousse G, Bonilla LF, Cotton F, Margerin L. Nonstationary stochastic simulation of strong ground motion time histories including natural variability: application to the K-Net Japanese database. Bulletin of the Seismological Society of America 2006;96:2103–17. https://doi.org/10.1785/0120050134.

[28] Vlachos C, Papakonstantinou KG, Deodatis G. A multi-modal analytical non-stationary spectral model for characterization and stochastic simulation of earthquake ground motions. Soil Dynamics and Earthquake Engineering 2016;80:177–91. https://doi.org/10.1016/j.soildyn.2015.10.006.

[29] Huang D, Wang G. Energy-compatible and spectrum-compatible (ECSC) ground motion simulation using wavelet packets. Earthq Eng Struct Dyn 2017;46:1855–73. https://doi.org/10.1002/eqe.2887.

[30] Tamhidi A, Kuehn N, Ghahari SF, Rodgers AJ, Kohler MD, Taciroglu E, et al. Conditioned simulation of ground-motion time series at uninstrumented sites using Gaussian process regression. Bulletin of the Seismological Society of America 2022;112:331–47. https://doi.org/10.1785/0120210054.

[31] Alimoradi A, Beck JL. Machine-learning methods for earthquake ground motion analysis and simulation. J Eng Mech 2015;141:04014147. https://doi.org/10.1061/(ASCE)EM.1943-7889.0000869.

[32] Safak E, Boore DM. On low-frequency errors of uniformly modulated filtered white-noise models for ground motions. Earthq Eng Struct Dyn 1988;16:381–8. https://doi.org/10.1002/eqe.4290160307.

[33] Rodolfo Saragoni G, Hart GC. Simulation of artificial earthquakes. Earthq Eng Struct Dyn 1973;2:249–67. https://doi.org/10.1002/eqe.4290020305.

[34] Burks LS, Baker JW. Validation of ground-motion simulations through simple proxies for the response of engineered systems. Bulletin of the Seismological Society of America 2014;104:1930–46. https://doi.org/10.1785/0120130276.

[35] Goulet CA, Abrahamson NA, Somerville PG, Wooddell KE. The SCEC broadband platform validation exercise: methodology for code validation in the context of seismic-hazard analyses. Seismological Research Letters 2015;86:17–26. https://doi.org/10.1785/0220140104.

[36] Olsen KB, Mayhew JE. Goodness-of-fit criteria for broadband synthetic seismograms, with application to the 2008 mw 5.4 Chino Hills, California, earthquake. Seismological Research Letters 2010;81:715–23. https://doi.org/10.1785/gssrl.81.5.715.

[37] Rezaeian S, Der Kiureghian A. Simulation of synthetic ground motions for specified earthquake and site characteristics. Earthq Eng Struct Dyn 2010;39:1155–80. https://doi.org/10.1002/eqe.997.